Structural Engineering and Mechanics, *Vol. 57, No. 6 (2016) 1051-1064*
DOI: http://dx.doi.org/10.12989/sem.2016.57.6.1051

Effect of stiffener arrangement on hysteretic behavior of link-to-column connections

Saman Zarsav[1a], Seyed Mehdi Zahrai[*2] and Asghar Vatani Oskouei[3b]

[1]*Islamic Azad University, Takestan Branch, Takestan, Iran*
[2]*School of Civil Engineering, The University of Tehran, Tehran, Iran*
[3]*Shahid Rajaee Teacher Training University, Tehran, Iran*

(Received May 6, 2015, Revised December 21, 2015, Accepted February 2, 2016)

Abstract. Link-to-column connections in Eccentrically Braced Frames (EBFs) have critical role in their safety and seismic performance. Accordingly, in this study, contribution of supplemental stiffeners on hysteretic behavior of the link-to-column connection is investigated. Considered stiffeners are placed on both sides and parallel to the link web between the column face and the first stiffener of the link. Hysteretic behaviors of the link beams with supplemental stiffeners are numerically investigated using a pre-validated numerical model in ANSYS. It turned out that supplemental stiffeners can change energy dissipation mechanism of intermediate links from shear-flexure to shear. Both rectangular and trapezoidal supplemental stiffeners are studied. Moreover, optimal placement of the supplemental stiffeners is also investigated. Obtained results indicate a discrepancy of less than 9% in maximum link shear of the numerical and experimental specimens. This indicates that the numerical results are in good agreement with those obtained from the test. Trapezoidal supplemental stiffeners improve rotational capacity of the link. Moreover, use of two supplemental stiffeners at both ends of the link can more effectively improve hysteretic behavior of intermediate links. Supplemental stiffeners would also alleviate the imposed demands on the connections. This latter feature is more pronounced in the case of two supplemental stiffeners at both ends of the link.

Keywords: link-to-column connections; supplemental stiffeners; cyclic behavior; plastic hinges; trapezoidal supplemental stiffeners

1. Introduction

Eccentrically Braced Frames (EBFs) are among the well-recognized lateral load resisting systems in which the inelastic action is restricted primarily to the ductile links. Some of the typical EBFs are arranged to have one end of the link connected to the column. In such configurations, the integrity of the link-to-column connection is essential to achieve a reliable performance. AISC 341 (AISC 341 2005) stipulates stringent provisions for EBFs to ensure that the inelastic behaviors would remain mainly within the links. It also requires qualification testing of link-to-column

∗Corresponding author, Professor, E-mail: mzahrai@ut.ac.ir
[a]M.Sc., E-mail: saman_zarsav@yahoo.com
[b]Associate Professor, E-mail: vatani@srttu.edu

http://www.techno-press.org/?journal=sem&subpage=8 ISSN: 1225-4568 (Print), 1598-6217 (Online)

connections to demonstrate that the required link plastic rotation can be achieved prior to the connection failure. The results of the previous experimental studies have indicated that some of the widely used connection details might experience premature failure (Okazaki *et al*. 2009). The AISC 341 has also acknowledged the present difficulties with link-to-column connections. Its commentary reminds engineers that this is a topic of ongoing research and suggests that it may be wise to avoid these connections altogether until a good solution is found. (Prinz and Richards, 2009)

Okazaki *et al*. (2004) have tested link-to-column connections under cyclic loading and reported the inelastic rotation capacity of links with various link-to-column connection details. Out of twelve W18x40 links, ten specimens experienced fracture of the link flanges near the connection at rotations from 0.007 to 0.07 rad. The specimen with a connection following the modified welding recommendations outlined in FEMA-350 (Federal Emergency Management Agency [FEMA] 2000) experienced fracture after 0.05 rad.

In previous studies, finite element models of EBF links have demonstrated good prediction of link behavior under cyclic loading. Richards and Uang (2005) have used finite element models of links to predict strength deterioration due to flange and web local buckling. Berman and Bruneau (2007) have also used finite element models to investigate the behavior of tubular links. Both of these studies have been carried out in parallel with experimental programs, providing opportunities for extensive model validation. The numerical models by Richards and Uang (2005) and Berman and Bruneau (2007) have resulted in hysteretic behavior and overall deformation patterns that were consistent with the experimental results by Arce (2002) and Berman and Bruneau (2007). In another analytical study, Prinz and Richards (2009) have evaluated performance of perforated EBF links with portions of the link web removed. They concluded that putting holes in the link web would reduce plastic strains in the link flanges near the connection.

In 2009, Okazaki *et al*. (2009) have proposed a pair of supplemental stiffeners at the link-to-column connection. The proposed stiffeners are placed on both sides of the link web between the column flange and the first link stiffener. These stiffeners which are parallel to the link web are intended to strengthen the connection. According to the experimental results (Okazaki *et al*., 2009), link-to-column connections with the supplemental stiffeners have shown superior rotation capacity which comply with the requirements of AISC 341. In addition, plastic hinge formation would be well restrained within the link away from the connection.

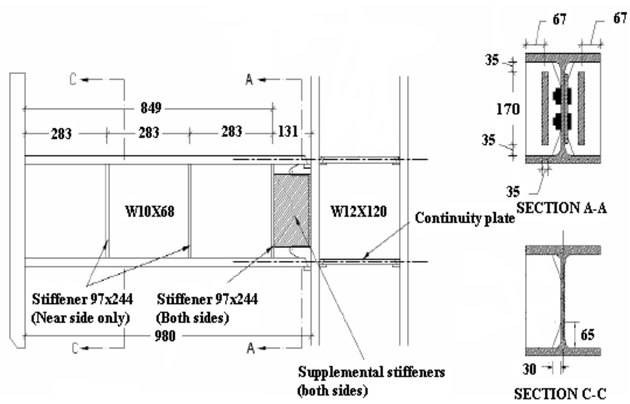

Fig. 1 AISC-6 specimen-overall layout

This paper discusses analytical study of the link to column connections with supplemental stiffeners. Supplemental stiffeners with different geometries are investigated to explore sensitivity of the rotational capacity to geometrical parameters of the stiffeners. It would be shown that arrangement of the supplemental stiffeners can change behavior of intermediate links to act similar to short links. This latter feature would be of interest from both architectural and structural points of view. The study begins by verifying the numerical model with comparing analytical results of finite element model of the short link specimen of AISC-6 (Fig. 1) with its corresponding experimental specimen of Okazaki *et al*. (2009) under cyclic loading. Furthermore, hysteretic behaviors of two specimens are compared with each other and the effect of geometrical change and the arrangement of the supplemental stiffeners on improving the performance of these EBFs are investigated.

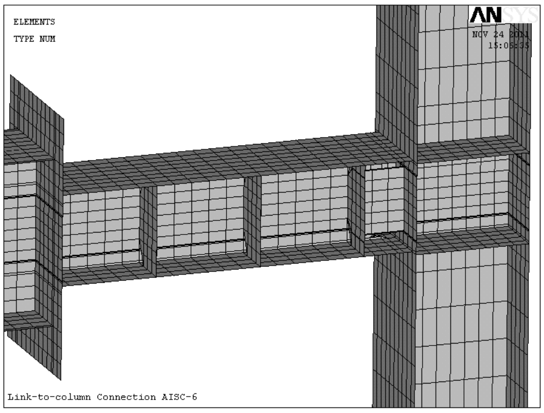

Fig. 2 Typical mesh details for AISC-6 specimen (Prinz and Richards 2009) (Dimensions in mm)

2. Modeling and verification

As the current study is devoted to numerical investigation of cyclic behavior of link-to-column connections with supplemental stiffeners, validity of the numerical model is examined by the experimental results obtained earlier by Okazaki *et al*. (2009). Adopted specimen has been called AISC-6 by Okazaki *et al*. (2009). To validate the model further, a similar experimental specimen of AISC-6 which was tested by Drolias (2007) is also considered during the verification phase of the study.

The experimental model is a sub-assemblage of a short link-to-column connection (Fig. 1) in which, web and flanges of the link beam are welded by full penetration welding to the column flange. Also full penetration weld is used for welding the supplemental stiffeners, from one side to the column flange and the other side to the first stiffener of the link. To transfer the shear force, a shear tab is used which is welded to the flange of column and bolted to the link web. The dimensions and geometry of the link beam, the beam outside the link, the column and the stiffeners are exactly modeled according to experimental specimen. As the link to column connection is of full penetration weld, the weld itself is not explicitly modeled and strain compatibility is assumed at the link-to-column interface.

Modeling in ANSYS software, is done by the SHELL43 element which has 4 nodes with 6 degrees of freedom at each node (Fig. 2). The element has plasticity, creep, stress stiffening, large deflection, and large strain capabilities. In order to increase accuracy of the model, finer meshes are used along the link beam and around the connection regions. Further details about the numerical model are illustrated in Fig. 3. As depicted in Fig. 3, displacement controlled cyclic loads are imposed at the bottom of the column. It should be noted that the weld access holes is carefully modeled according to the dimension of MW connection (incorporated modifications in welding recommended in FEMA) weld access hole in the study performed by Okazaki *et al*. in 2006 (Fig. 4). MW is a connection that contains weld metal with notch toughness requirement. This connection adopts the modifications in welding which are currently widely accepted for moment connections (Okazaki *et al*. 2004).

As depicted in Fig. 5, adopted loading protocol is the one proposed by Richards and Uang (2004) which has been exclusively developed for short link beams. Table 1 represents further details about the imposed displacements and the corresponding link rotations.

In the numerical model, four kinds of steel for different parts of the sub-assemblage are used with their yield, f_y, and ultimate, f_u, stresses presented in Table 2. These mechanical parameters are similar to those measured during the experiments (Okazaki *et al*., 2004). The behavior of steel is

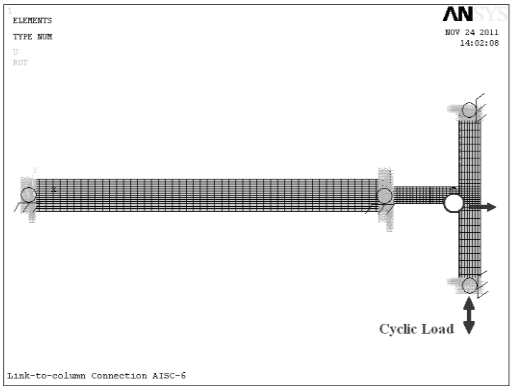

Fig. 3 Loading details and numerical model

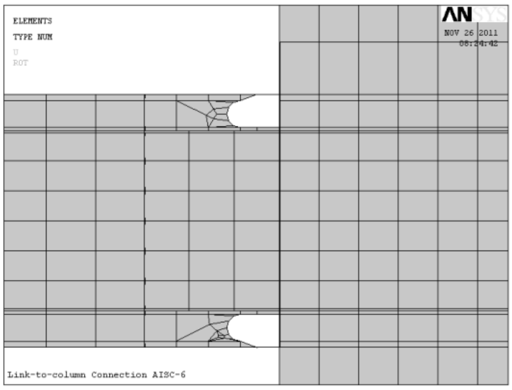

Fig. 4 Weld access hole modeling details and displacement constrains

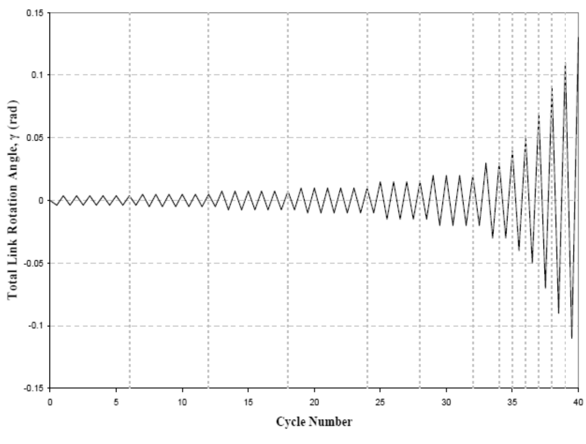

Fig. 5 Adopted loading protocol

Table 1 Adopted loading protocol

Load step	Total link rot. angle (rad)	Number of cycles	Column vertical displacement (mm)
1	±0.00375	6	±3.675
2	±0.005	6	±4.9
3	±0.0075	6	±7.35
4	±0.01	6	±9.8
5	±0.015	4	±14.7
6	±0.02	2	±19.6
7	±0.03	2	±29.4
8	±0.04	1	±39.2
9	±0.05	1	±49
10	±0.07	1	±68.6
11	±0.09	1	±88.2
12	±0.11	1	±107.2
13	±0.13	1	±127.4

Table 2 Section properties for the column and the link

Section	f_y (kN/mm^2)		f_u (kN/mm^2)	
	Flange	Web	Flange	Web
Column (W12x120)	0.323	0.353	0.455	0.485
Link (W10x68)	0.319	0.404	0.479	0.531

modeled using Von Mises yielding criteria with kinematic hardening. Elastic modulus of 200 GPa and Poisson ratio of 0.3 are also considered for the steel material

Adopted set-up for the experiments was designed to impose both forces and displacements to the link beam near the connection, in the sub-assemblage. Fig. 6(a) shows the energy dissipation mechanism in the EBF. Fig. 6(b) is also the schematic representation of the test setup.

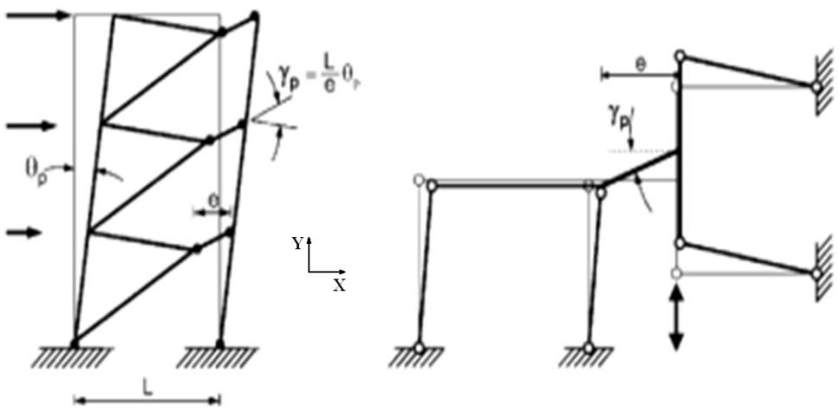

Fig. 6(a) Energy dissipation Mechanism of EBF (b) Schematic representation of test setup (Okazaki and Engelhardt 2007)

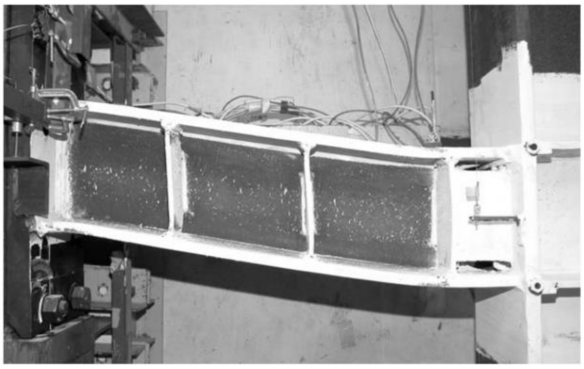

Fig. 7 (a) AISC-6 specimen, last full loading cycle prior of failure (Drolias 2007)

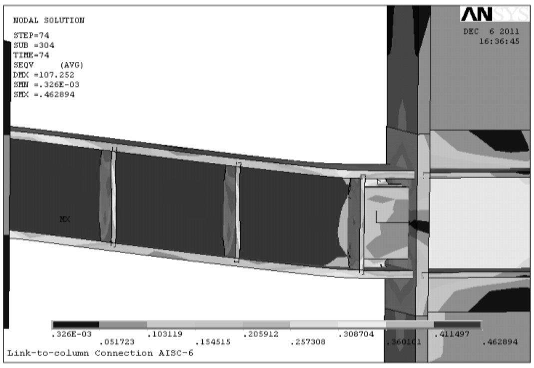

(b) Finite elementAISC-6 Specimen Von Mises stress($\frac{KN}{mm^2}$) last full loading cycle

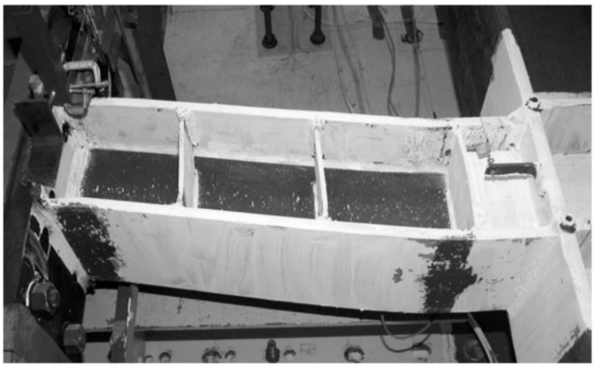

Fig. 8 (a) AISC-6 specimen, yielding confined in the unreinforced portion (Drolias 2007)

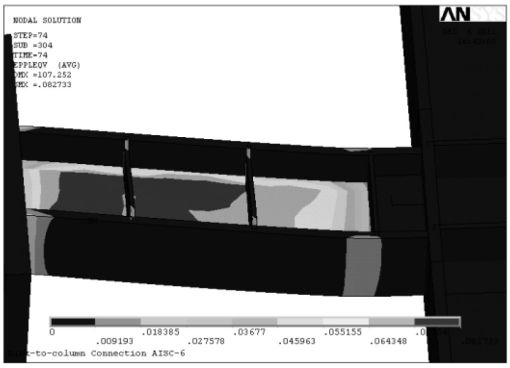

(b) Finite elementAISC-6 Specimen, Von Mises plastic strain in last loading cycle

The experimental specimen of AISC-6 is compared with its numerical counterpart in Fig. 7. Fig. 7(a) shows the experimental specimen during the last load reversal before failure. Except the first panel of the link beam strengthened by the supplemental stiffeners, the entire short link beam web is yielded which is a desirable outcome.

Moreover it is observed that by strengthening the first panel of the link beam with the supplemental stiffeners, the plastic hinge moves into the link beam and subsequently the stress demands near the link-to-column connection would be decreased. All of these characteristics are also clear from the numerical specimen (Fig. 7(b)).

Fig. 8(a) illustrates flange yielding of the link close to the supplemental stiffeners in the test specimen. This indicates that plastic hinge has been formed after the first panels of the link beam strengthened by the supplemental stiffeners. This behavior is also observed in the finite element model of the specimen (Fig. 8(b)). In Fig. 9(a), it is shown that in test specimen, the failure happened due to the web fracture of the link at the third panel after the supplemental stiffeners. Again the same result is obtained from the numerical specimen where the maximum equivalent plastic strain is developed at the same point as the test specimen fractured. (Fig. 9(b))

The hysteresis curves obtained from the test and the finite element specimens are shown in Fig. 10. Note that the experimental hysteretic behavior is presented in terms of inelastic rotation while

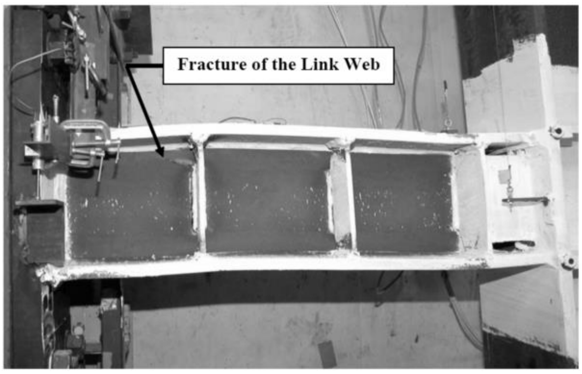

Fig. 9 (a) AISC-6 specimen, yielding confined in the unreinforced portion (Drolias 2007)

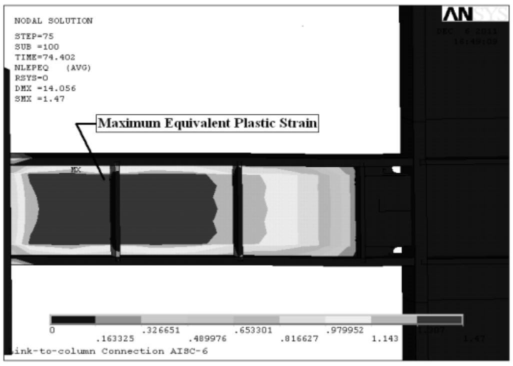

(b) Finite elementAISC-6 Specimen, Von Mises plastic strain last full loading cycle

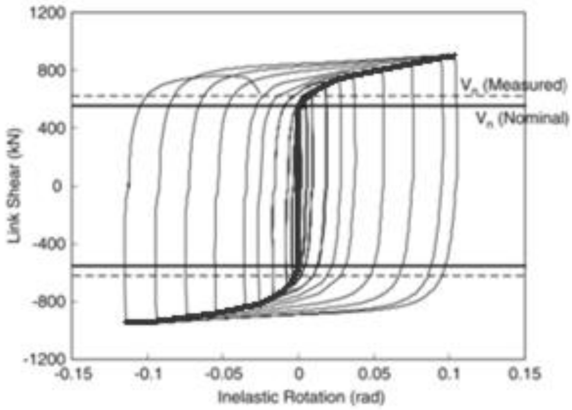

Fig. 10(a) Hysteresis curve (Shear-Inelastic rotation) AISC-6 test specimen (Okazaki *et al*. 2009)

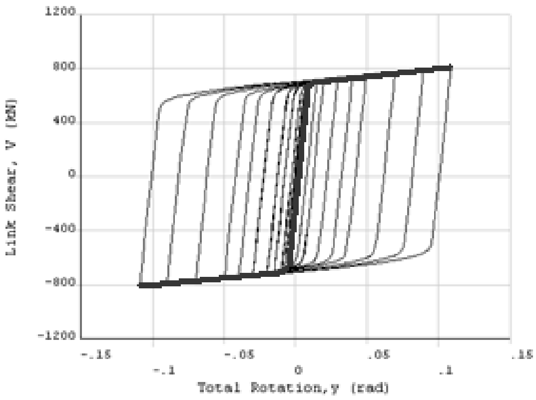

(b) Hysteresis curve (Shear-Total rotation) AISC-6 ANSYS output

the numerical hysteretic behavior illustrates the response in terms of the total (elastic+inelastic) link rotation. It can be seen that the numerical behavior is in good agreement with the experimental one. In the study performed by Okazaki *et al*. (2009), the maximum developed shear in the link beam in AISC-6 specimen is 890 kN and this value in the finite element specimen is 812 kN. As a result the difference is less than 9% which is in an acceptable range. According to Figs. 7 to 10, it can be seen that the numerical specimen can reliably simulate hysteretic behavior of its experimental counterpart.

3. T-AISC-6 specimen and comparison with AISC-6

T-AISC-6 specimen is similar to AISC-6 except that the trapezoidal supplemental stiffeners are used instead of the rectangular ones (Fig. 11). Other details including material, loading protocol, modeling techniques are similar to those of the AISC-6 specimen. In Fig. 12, the hysteresis curves of the two specimens are shown. It can be observed that the hysteretic behaviors of both specimens are rather the same.

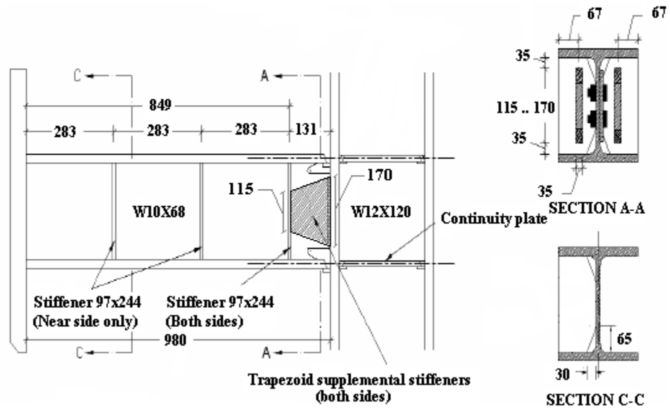

Fig. 11 T-AISC-6 specimen-Overall layout (Dimensions in mm)

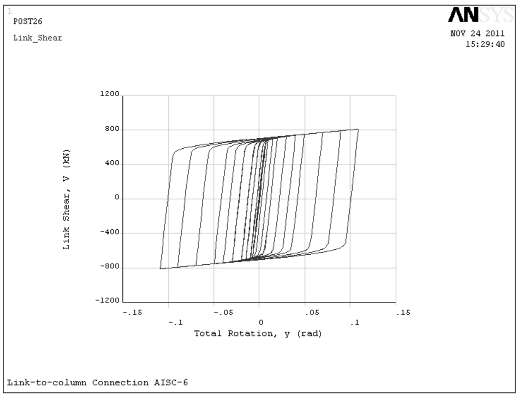

Fig. 12(a) Hysteresis curve (Shear-Total rotation)

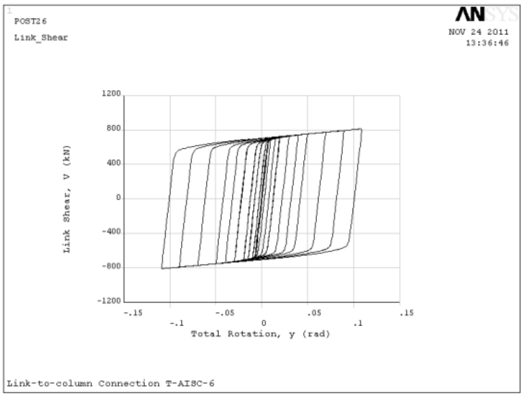

(b) Hysteresis curve (Shear-Total rotation)

In addition to the cyclic displacements, an upward force of 810 kN is applied to the bottom of the column to investigate stiffness of the link beam specimens.

Fig. 13, shows behavior of the specimens after applying the upward load of 810 kN. This force would result in displacements of 112.8 mm and 110.9 mm for the T-AISC-6 and AISC-6 specimens, respectively. In other words, the T-AISC-6 specimens would experience rotation angle of 0.115 rad while this value for the AISC-6 specimen is 0.113 rad. As a result, trapezoidal supplemental stiffeners could result in a link beam with improved flexibility, the feature that might be desirable in terms of energy dissipation capability.

4. Intermediate link beams with supplemental stiffeners

Regarding the architectural requirements in structures such as the existence of large openings in the frames, especially in interior frames, bracings can be transferred from the exterior frames to the interior frames and EBF with link next to column can be utilized. In some cases link beams with intermediate length are inevitable. Due to the Guideline of AISC-2005 about more desirable behavior of the short link beam (shear link), in this section a solution for changing the intermediate

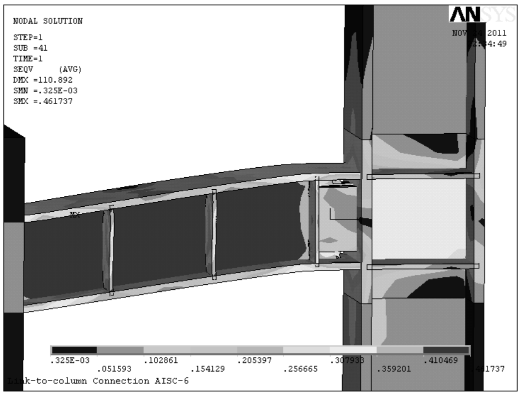

Fig. 13 (a) Von Mises stress ($\frac{KN}{mm^2}$)after loading AISC-6 specimen

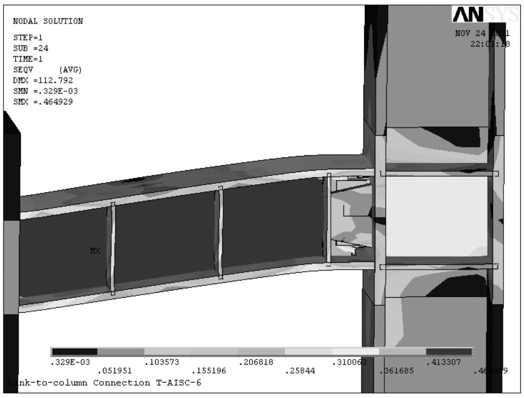

(b) Von Mises stress($\frac{KN}{mm^2}$) after loading T-AISC-6 specimen

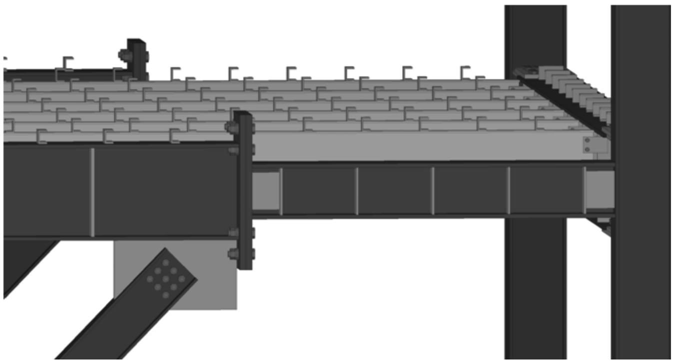

Fig. 14 Proposing different section for link and beam outside of the link (Overall layout)

links to short links is proposed to use two different sections for link beam and the beam outside of the link. As depicted in Fig. 14, these two elements would be connected to each other with end-to-end plates and high strength friction bolts. In this section two intermediate link beams are considered, namely specimens 1-I-AISC-6 and 2-I-AISC-6. The former has supplemental stiffeners only at one end, while the latter specimen has supplemental stiffeners at both ends (Fig. 15).

4.1 Proposed details for the specimens

Modeling and the used steel and applied loading protocol are similar to those used for the AISC-6 specimen in the previous section. However, considered specimens in this section have intermediate link lengths which are longer than that of the AISC-6 specimen.

As illustrated in Fig. 15(a), the 1-I-AISC-6 specimen has a total link length of 1270 mm. length of the supplemental stiffener is 131 mm and the active length of the link would be 1139 mm. meanwhile, the specimen 2-I-AISC-6 has an active link length of 1008 mm due to the fact that it contains two supplemental stiffeners at both ends (Fig. 15(b)). Note that the active length is the length between two end points of the supplemental stiffeners.

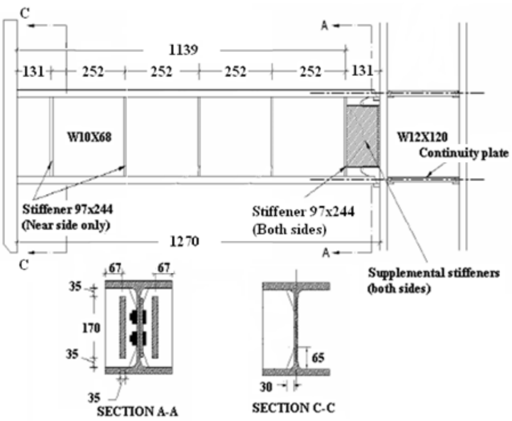

Fig. 15 (a) (1-I-AISC-6) Specimen Overall layout (Dimensions in mm)

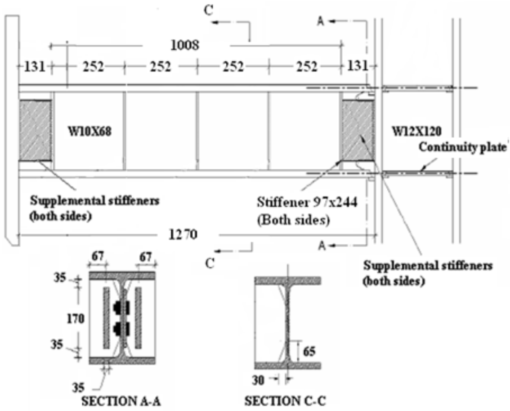

(b) (2-I-AISC-6) Specimen Overall layout (Dimensions in mm)

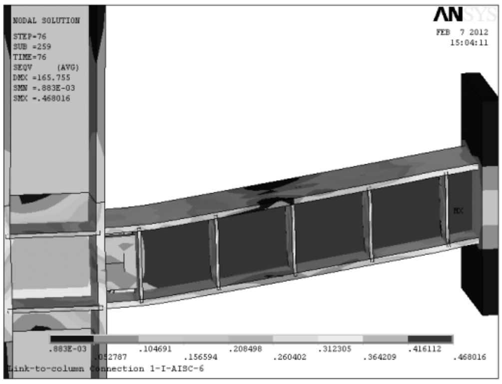

Fig. 16 (a) Von Mises Stress($\frac{KN}{mm^2}$) (1-I-AISC-6) Specimen at last full loading cycle

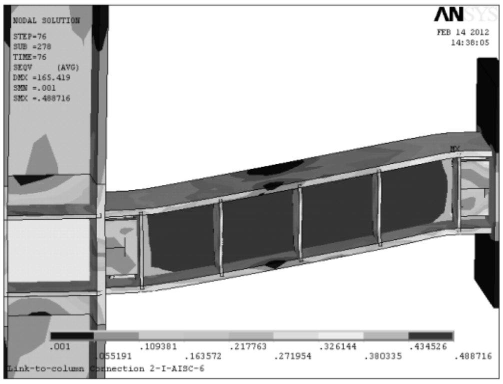

(b) Von Mises Stress ($\frac{KN}{mm^2}$) of (2-I-AISC-6) Specimen at last full loading cycle

4.2 Behavioral comparison of the specimens 1-I-AISC-6 and 2-I-AISC-6

As shown in Fig. 16, the maximum stress in the link web of the specimens 1-I-AISC-6 and 2-I-AISC-6 are 0.468 and 0.488 kN/mm^2, respectively. That is, two supplemental stiffeners at both ends of the 2-I-AISC-6 specimen lead to 4% increase in the developed stresses. Moreover, two supplemental stiffeners have reduced the imposed demands on the regions close to the beam-to-link connection. This behavior is also obvious from the developed strains in Fig. 17. In other words, implementing two supplemental stiffeners would guarantee plastic hinge formation away from the link-to-column and link-to-beam connections.

Regarding the Von Mises total mechanical strains of the specimens, the maximum Von Mises strain in 2-I-AISC-6 specimen is increased about 27% which indicates improved energy dissipation capability of this specimen. Moreover, from Fig. 17, it can be observed that in 1-I-AISC-6 specimen the maximum strain is developed at the region close to the link-to-beam connection. Such strain distribution can cause weld fracture at the link flange to the end plate connection. On the other hand, such strain distribution is not the case for the 2-I-AISC-6 specimen

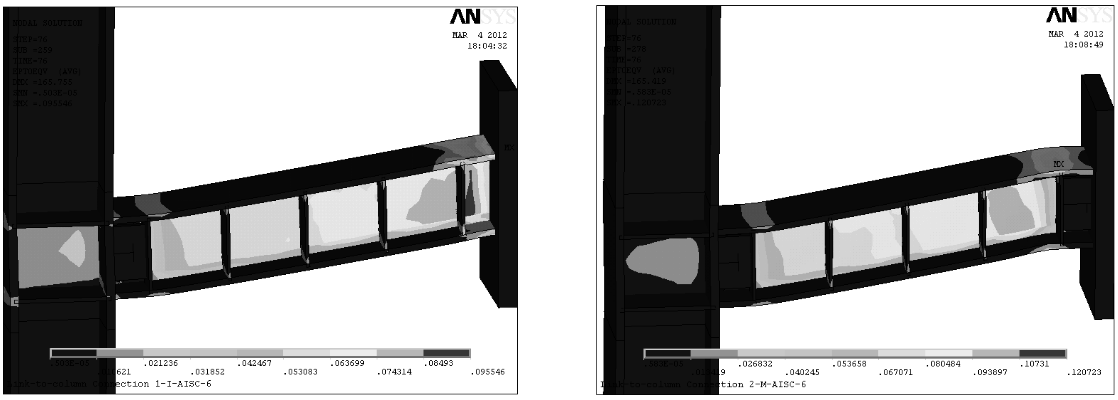

Fig. 17 (a) Von Mises total mechanical strain of (1-I-AISC-6) Specimen

(b) Von Mises total mechanical strain of (2-I-AISC-6) Specimen

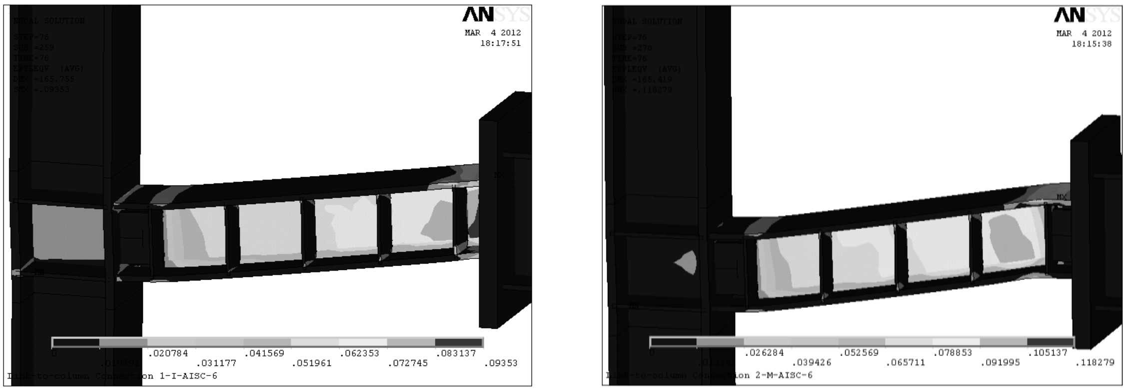

Fig. 18 (a) Von Mises plastic strain of (1-I-AISC-6) Specimen

(b) Von Mises plastic strain of (2-I-AISC-6) Specimen

due to the used supplemental stiffeners at both ends.

Fig. 17(a) indicates that the fracture of 1-I-AISC-6 specimen would occur close to the first main stiffener of link web. However, in the case of 2-I-AISC-6 specimen, the fracture zone would be shifted toward the middle of the link at the second panel. Fig. 17(b) clearly has shown the transition of plastic hinges inward the ink beam. From Fig. 18, it is clear that the propagation of plastic strains to the force controlled elements (connections and column) is more pronounced in the case of 1-I-AISC-6 specimen. According to the so called capacity design procedure, plastic strains should be confined within the intended fuse, which is the link beam in the case of EBF. As a result, from capacity design point of view, link beams with supplemental stiffeners at both ends would reveal superior behavior.

Hysteretic behaviors of both specimens are shown in Fig. 19. Maximum developed shears in the specimens 1-I-AISC-6 and 2-I-AISC-6 are 783 kN and 817 kN, respectively. As a result, more energy has been dissipated by the latter specimen. By re-drawing the hysteretic curve according to the active link length of the specimens, superior behavior of the specimen 2-I-AISC-6 with two supplemental stiffeners would be better clarified. This is shown in Fig. 20. Note that in Figs. 19 and 20, e_{total} refers to the total length of the link beam, while e_{active} represents the active part of

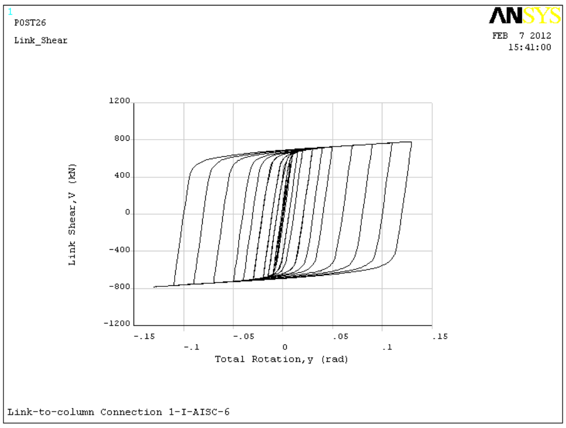

Fig. 19 (a) Hysteresis curves of 1-I-AISC-6 (Shear-Total Rotation based on e_{total} =1270 mm)

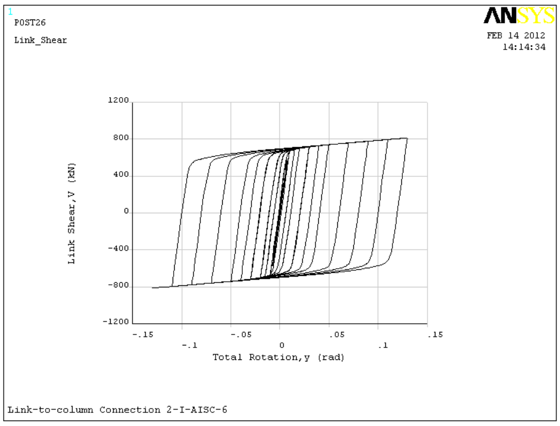

(b) Hysteresis curves of 2-I-AISC-6 (Shear-Total Rotation based on e_{total} =1270 mm)

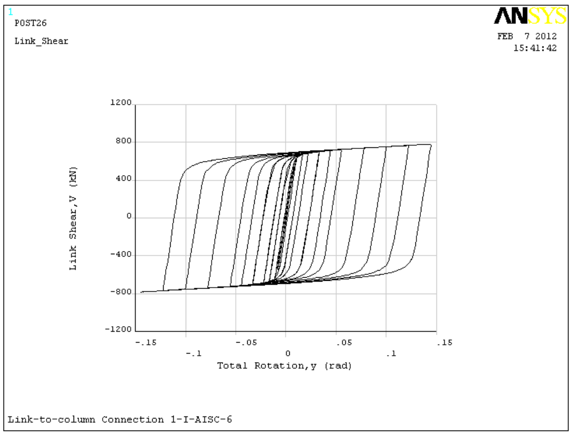

Fig. 20 (a) Hysteresis curves of 1-I-AISC-6 (Shear-Total Rotation based on e_{active} =1139 mm)

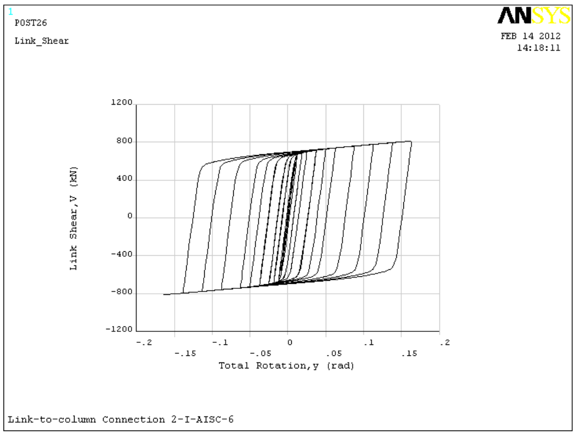

(b) Hysteresis curves of 2-I-AISC-6 (Shear-Total Rotation based on e_{active} =1008 mm)

the link beam which demonstrates plastic behavior and contributes to energy dissipation.

Utilizing different sections in link beam and beam outside of the link leads to the following advantages: the possibility of workshop welding, supervisions on welding the link to column connections, easy installation of Tree-Column structures and the possibility of utilizing a link with a different section from the main beam (a section smaller than the main beam).

There are two recommendations regarding the erection of such sections: 1) joists should be parallel to the link-beam direction to erect the joists and beams at the same construction sequence, and 2) regarding the requirement of plastic rotation of the link beam and its freedom of motion during a design level earthquake, joists and floor diaphragm should impose minimal constraint for the link beam (Fig. 14).

A summary of all results obtained in the current study is represented in Table 3.

Table 3 Numerical modeling results

Specimen	Supplemental stiffeners type	Link type	e_{total} (mm)	e_{active} (mm)	Loading methods	Rotation angle	Last full loading cycle		
							Link Shear (kN)	Link web stress (kN/mm^2)	Von mises strain
AISC-6	Rectangular 244×97 mm	short	980	849	Pushover	0.113	--	--	--
T-AISC-6	Trapezoidal 244×94×115 mm	short	980	849	Pushover	0.115	--	--	--
1-I-AISC-6	Rectangular one end, 244×97 mm	intermediate	1270	1139	Cyclic	0.165	783	0.468	0.095
2-I-AISC-6	Rectangular both end, 244×97 mm	intermediate	1270	1008	Cyclic	0.165	817	0.488	0.121

5. Conclusions

The main findings and achievements of this study can be listed as following,

• A numerical model for the short link specimen AISC-6 is obtained and verified with earlier experimental results. Obtained results indicate that the numerical model can simulate hysteretic behavior of the link beam with good accuracy.

• Compared to the rectangular supplemental stiffeners, trapezoidal supplemental stiffeners would result in a more ductile link beam with improved rotational capacity.

• For more appropriate performance of the EBF frame with the link beam connected to the column, different cross sections can be used for the link beam and the beam outside of the link.

• Use of two supplemental stiffeners at both ends of the link beam would increase shear capacity of the link by about 4%.

• Supplemental stiffeners at the both ends of link beam cause formation of plastic hinges away from the end connections. In this way, reduced stress demands would be imposed on the end connections (link-to-column and link-to-beam connections).

• Supplemental stiffeners at both ends of intermediate link beam can change behavior of the link from flexure-shear to shear behavior. Accordingly the intermediate link, which is desirable from architectural view, would act similar to a short link, which is desirable from structural point of view. So supplemental stiffeners can be used for intermediate link beams to meet the structural and architectural requirements simultaneously.

References

American Institute of Steel Construction, Inc. (AISC) (2005), Seismic Provisions for structural steel buildings, Standard ANSI/AISC 341-05, Chicago, IL.

Arce, G. (2002), "Impact of higher strength steels on local buckling and overstrength of links in eccentrically braced frames", M.Sc. Thesis, Univ. of Texas at Austin, Austin.

Berman, J.W. and Bruneau, M. (2007), "Experimental and analytical investigation of tubular links for eccentrically braced frames", *Eng. Struct*., **29**(8), 1929-1938.

Drolias, A. (2007), "Experiments on link-to-column connections in steel eccentrically braced frames", M.Sc. Thesis, Department of Civil Engineering, University of Texas at Austin, Austin.

Federal Emergency Management Agency (FEMA) (2000), Recommended seismic design criteria for steel moment-frame buildings, Publication FEMA-350, Washington DC.

Okazaki, T., Engelhardt, M., Drolias A., Schell, E., Hong, J. and Uang, C. (2009), "Experimental investigation of link-to-column connections in eccentrically braced frames", *J. Constr. Steel Res*., **65**(7), 1401-1412.

Okazaki, T. and Engelhardt, M. (2007), "Cyclic loading behavior of EBF links constructed of ASTM A992 steel", *J. Constr. Steel Res*., **63**(6), 751-765.

Okazaki, T., Engelhardt, M.D., Nakashima, M. and Suita, K. (2006), "Experimental performance of link-to-column connections in eccentrically braced frames", *J. Struct. Eng*., **132**(8), 1201-1211.

Okazaki, T., Engelhardt, M., Nakashima, M. and Suita, K. (2004), "Experimental study on link-to-column connection steel eccentrically braced frames", *13th World Conference on Earthquake Engineering*, Vancouver, Canada, August.

Prinz, G.S. and Richards, P. (2009), "Eccentrically braced frame links with reduced web sections", *J. Constr. Steel Res*., **65**(10-11), 1971-1978.

Richards, P.W. and Uang, C.M. (2005), "Effect of flange width thickness ratio on eccentrically braced frame link cyclic", *J. Struct. Eng*., **131**(10), 1546-1552.

Richards, P. and Uang, C.M. (2004), "Development of testing protocol for links in eccentrically braced frames", *13th World Conference on Earthquake Engineering*, Vancouver, Canada, August.

PL